

Nanostructures Technology, Research and Applications

Academic and Research Staff

Prof. Karl Berggren, Dr. Rajesh Menon, Mark. K. Mondol, Dr. Euclid Moon Dr. Mark L. Schattenburg, Prof. Henry I. Smith,

Visiting Scientists, Postdoctoral Associates and Research Affiliates

Dr. Timothy Savas,

Graduate Students

Vikas Anant, Will Arora, Bryan Cord, Eric Dauler, Corey Fucetola, Charles Holzwarth, Xiaolong Hu, Jan Kupec, Joshua Leu, Anthony Nichols, Tom O'Reilly, Amil Patel, Thomas Reisinger (visiting), Carlos Ruiz (visiting), Jie Sun, Hsin-Yu Tsai, Donald Winston, Joel Yang,

Collaborators

Prof. Mark Baldo, Prof. George Barbastathis, Dr. Fernando Castano, Prof. Jesus DelAlamo, Prof. Judy Hoyt, Prof. Erich Ippen, Prof. John Kasakian, Prof. Franz Kaertner, Prof. Leslie Kolodziejwski, Dr. Jagadeesh Moodera, Prof. Rajeev Ram, Prof. Caroline Ross, Prof. Edwin L. Thomas, Prof. Carl Thompson.

Technical and Support Staff

James Daley, Tiffany Kuhn

1. Nanostructures Laboratory

The NanoStructures Laboratory (NSL) at MIT develops techniques for fabricating surface structures with feature sizes in the range from nanometers to micrometers, and uses these structures in a variety of research projects. The NSL is closely coupled to the Space Nanotechnology Laboratory (SNL) with which it shares facilities. The NSL and SNL include facilities for lithography (photo, interferometric, electron-beam, imprint, and x-ray), etching (chemical, plasma and reactive-ion), liftoff, electroplating, sputter deposition, and e-beam evaporation. Much of the equipment, and nearly all of the methods, utilized in the NSL/SNL are developed in house. Generally, commercial lithography and processing equipment, designed for the semiconductor industry, cannot achieve the resolution needed for nanofabrication, is inordinately expensive, and lacks the required flexibility for our research. This report does not cover all of the research conducted in the NSL facilities, but instead focuses on those that advance the state of the art of nanofabrication and are under Prof. Henry I. Smith.

2. Scanning-Electron-Beam Lithography (SEBL) Facility

Sponsors:

MIT Institute facility under RLE

Project Staff:

Mark K. Mondol, Dr. Feng Zhang, Prof. Henry I. Smith, Prof. Karl Berggren

In 2004, the Nanostructures Lab converted its scanning-electron-beam-lithography (SEBL) facility in Room 38-165 into an Institute-wide service facility under the Research Laboratory of Electronics (RLE). This facility provides MIT and outside users with easily accessible e-beam lithography, coupled with resident expertise and advice. The facility is managed by Mark Mondol who provides training on the e-beam tools, direct patterning service, and advice on optimal nanofabrication techniques and strategies. The NanoStructures Laboratory (NSL) and the

Microsystems Technology Laboratories (MTL) have service facilities for spin coating of resists, resist development and other forms of processing.

Projects that made use of the SEBL facility during the past year included: patterned nanotube growth; relief templates for self assembly of block copolymers; point-contact devices; 1-D and 2-D photonic crystals; ring-resonator add/drop filters; optical-polarization splitter-rotator devices; novel liquid-crystal devices; magnetic-memory devices; quantum photodetectors; templates for nanoimprint lithography; photomasks for interferometric-spatial-phase-imaging alignment and gapping; 4-point contacts for measurements on nanotubes and nanowires; III-V compound T-gate HEMTs and arrays of Fresnel zone plates. Research in lithographic processing included extreme cold development of PMMA and novel developer solutions for HSQ which demonstrated improved resolution and contrast. Use of the facility, by the MIT community, was widespread, there were: 25 Principal Investigators, 7 Departments, 8 Labs or Centers, 2 non-MIT entities and 45 distinct trained users over the last year.

Two SEBL tools are available. The Raith Turnkey 150 system is shown in Figure 1. Its electron-optical column is essentially identical to that of a Zeiss Gemini SEM, and provides a beam diameter as fine as 2 nm. Linewidths of ≤ 9 nm have been written with the system, as illustrated in Figure 2. The Raith 150 includes a pattern generator and laser-interferometer-controlled stage with an integrated software package which was upgraded to version 4.0 in the past year. This upgrade improved writing speed and system stability. Version 4.0 software now allows users to do automated field alignment to approximately ± 25 nm. The system can operate from 1 to 30keV accelerating voltage. Wafers up to 150 mm can be loaded into the system. Typically, users are trained for 3 to 10 hours and then allowed to operate the tool on their own. The tool is available, for most users, 24 hours a day, 7 days a week.

Figure 3 is a photograph of the VS-26 system. This instrument was put together at MIT from two systems (VS-2A and VS-6) obtained as gifts from IBM in the mid 1990's. VS-26 has a minimum beam diameter of about 10 nm. It operates at a fixed accelerating voltage of 50keV. Conversion software has been developed which allows a CAD data file to be fractured and translated prior to exposure, additional software was developed to generate arbitrary arcs. Substrates up to 200 mm diameter can be exposed at linewidths down to ~ 30 nm. However, the area available for patterning is limited to 95x95 mm.

The Raith 150 is used in a program to develop spatial-phase-locked e-beam lithography, described elsewhere. The objectives of that program are to achieve sub-1 nm pattern-placement accuracy, and to reduce the cost and complexity of SEBL. In a conventional SEBL system costing several million dollars, pattern placement accuracy is typically much worse than 10 nm.

The SEBL facility encourages users with a variety of experience levels and requirements. Experienced users are able to carry out complex, multilevel aligned exposures on the Raith-150 tool. Less experienced users get hands-on instructions from facility staff, and guidance during the learning and initial fabrication stages.

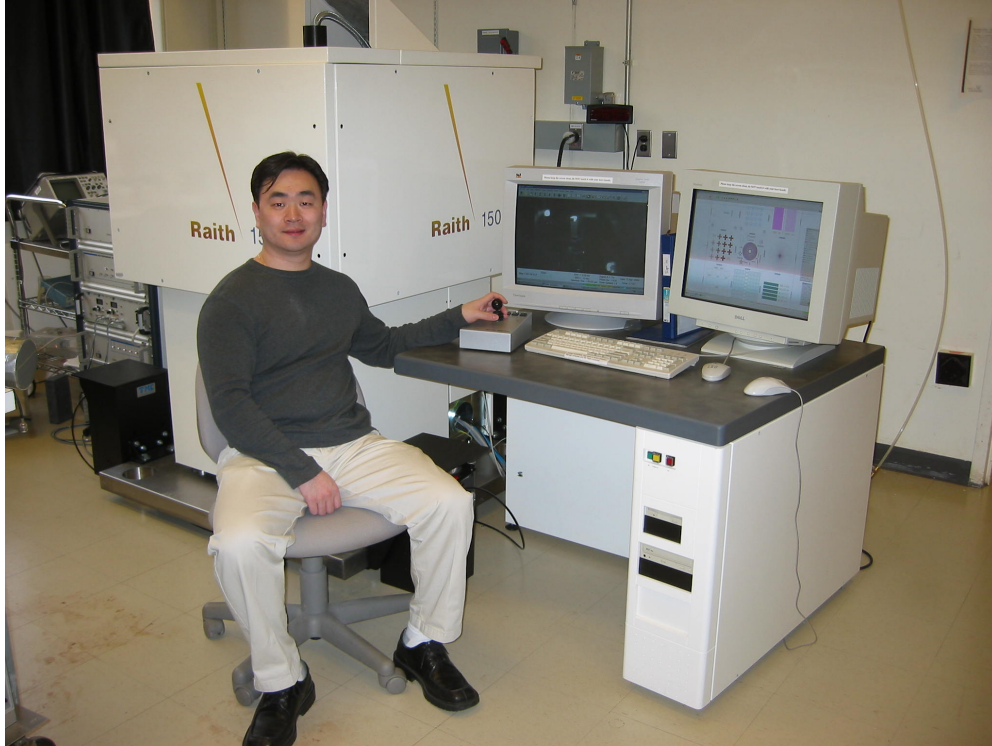


Figure 1. The Raith-150 electron-beam lithography system. This tool provides sub-20-nm patterning resolution, and pattern-placement accuracy ~ 1 nm via spatial phase locking. The operator is Dr. Feng Zhang.

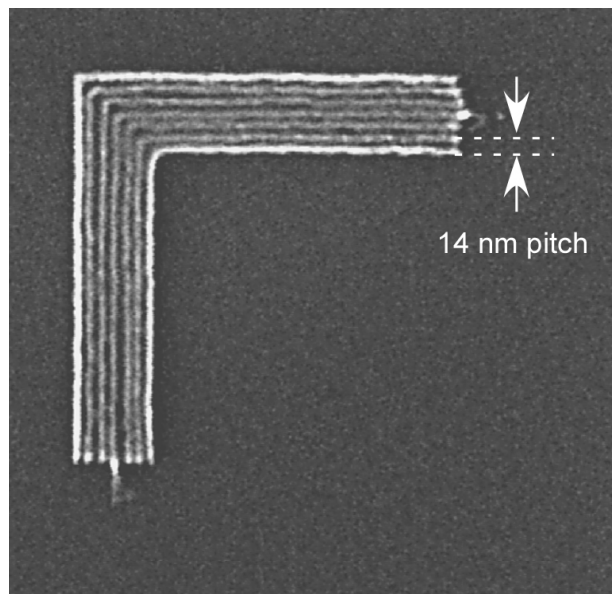


Figure 2: Scanning-electron micrograph of exposed and developed HSQ illustrating the resolution of the Raith 150 SEBL system. (J. K. W. Yang and K. K. Berggren, "Using High-Contrast Salty Development of Hydrogen Silsesquioxane for Sub-10-nm-Half-Pitch Lithography," *Journal of Vacuum Science & Technology B*, submitted for publication (2007))



Figure 3. Photograph of the VS-26 scanning-electron-beam lithography system.

3. Spatial-Phase-Locked Electron-Beam Lithography

Sponsors

National Science Foundation

Project Staff

Dr. Euclid E. Moon, Prof. Henry I. Smith, Prof. J. Todd Hastings (U. Kentucky)

Our research in spatial-phase-locked electron-beam lithography (SPLEBL) is conducted in collaboration with the University of Kentucky. It is aimed at reducing pattern-placement errors in electron-beam-lithography systems to the sub-1 nm level. Such high precision is essential for certain applications in photonics and nanoscale science and engineering. SPLEBL is currently the only approach capable of achieving such pattern-placement accuracy. As shown in Fig. 1, SPLEBL uses a periodic signal, derived from the interaction of the scanning e-beam with a fiducial grid placed directly on the substrate, to continuously track the position of the beam while patterns are being written. Any deviation of the beam from its intended location on the substrate is sensed, and corrections are fed back to the beam-control electronics to cancel beam-position errors. In this manner, the locations of patterns are directly registered to the fiducial grid on the substrate.

The research effort at MIT is now focused on developing the materials and processes for producing the fiducial grid, with the objectives of: maximizing the signal-to-noise of the secondary-electron signal derived from the grid; minimizing electron scattering from the grid,

which would be deleterious to precision lithography; maximizing the area and absolute accuracy of the grid; and minimizing the cost and inconvenience of producing the grid on substrates of interest. We have determined that signal levels are maximized when the grid is formed from nanoparticles. Substrates have been patterned with in-situ Faraday cups, as illustrated in Fig. 2, to make accurate measurements of signal-to-noise for a wide variety of nanoparticle types. To minimize electron scattering, the nanoparticles must be composed of low-atomic-number materials. Fullerenes may be the optimal nanoparticle, but achieving uniform thickness of layers and attaching the fullerenes along the grid lines represents a challenge of attachment chemistry. Scanning-beam interference lithography will be used to produce master grids. A special form of imprint lithography that maintains long-range spatial-phase coherence will be used to transfer attachment-chemistry grid patterns onto substrates of interest. The research effort at the University of Kentucky is focused on processing of the signal from the grid. Previous approaches utilized only the raster-scan mode. New approaches are being developed that enable spatial-phase locking while e-beam writing is conducted in a vector-scan mode.

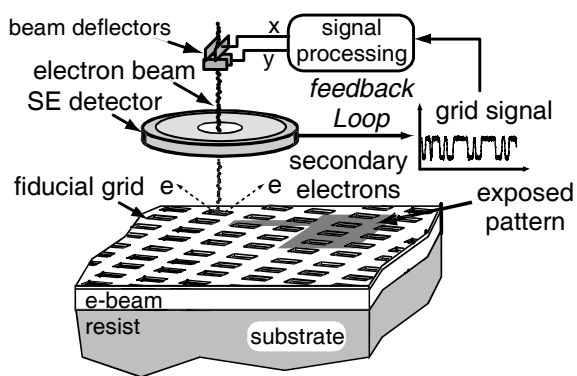


Figure 1: Schematic of the global-fiducial-grid mode of spatial-phase-locked electron-beam lithography. The periodic signal detected from the fiducial grid, which includes both X and Y components, is used to measure placement error, and a correction signal is fed back to the beam deflection system.

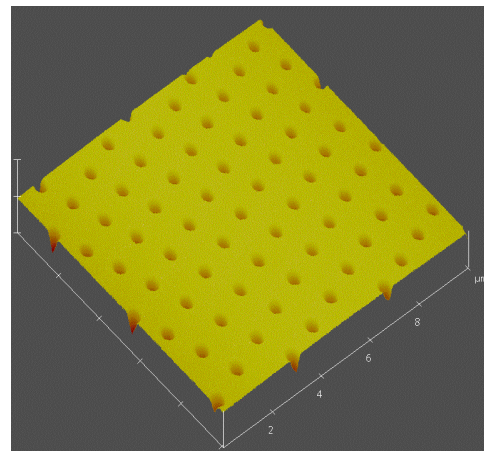


Figure 2: AFM scan of in-situ Faraday cups used to measure signal-to-noise for a variety of nanoparticles forming fiducial grids.

References

- [1] J.T. Hastings, F. Zhang, and H.I. Smith, "Nanometer-level stitching in raster-scanning e-beam lithography using spatial-phase locking," *J. Vac. Sci. Technol. B*, **21**, 2650 (2003).
- [2] F. Zhang, H.I. Smith and J.F. Dai, "Fabrication of high-secondary-electron-yield grids for spatial-phase-locked electron-beam lithography," *J. Vac. Sci. Technol. B*, **23**, 3061 (2005).

4. Imprint Lithography

Sponsors:

Internal funds

Project Staff:

Dr. Euclid E. Moon, Prof. Karl K. Berggren, Prof. Henry I. Smith

Imprint lithography is a straightforward and reliable means of replicating patterns from a template with feature sizes below 10 nm. Experiments have also demonstrated replication of features at the single-molecule level. Typically, the imprint template consists of a thick, fused-silica blank coated with 100 nm of hydrogen silsesquioxane (HSQ), patterned by scanning-electron-beam lithography (SEBL). The patterned template is treated with a release-assist agent such as alkyltrichlorosilane, which reduces the surface free energy of the template, and ensures that the template can be removed cleanly after imprint. A planarization layer material is spun on a silicon wafer, followed by nanoliter droplets of a low-viscosity etch-barrier fluid. The template is leveled and brought into proximity with the substrate. Upon contact, the etch barrier fluid distributes itself by capillary action throughout the cavities in the template pattern. Low pressure is applied to the template, slightly compressing the etch barrier fluid, and allowing a three-point force measurement around the periphery of the template to ensure proper leveling. The gap between the template and substrate is maintained at ~100 nm, which allows freedom of movement of the template parallel to the substrate, with the etch barrier fluid acting as a lubricating layer. Alignment is performed to the ~1-nm level using our novel Interferometric-Spatial-Phase Imaging (ISPI) alignment technology. A brief exposure of the etch barrier fluid to ultraviolet light initiates crosslinking of monomers in the fluid, after which the template is removed in a measured and level manner. The pattern remaining in the solidified etch barrier material is transferred into the substrate with a bi-layer reactive-ion etch.

Two custom-designed imprint lithography systems are in the NanoStructures Laboratory (NSL), one of which is illustrated in Fig. 1. The system can imprint on wafers up to 200 mm diameter, in field sizes up to 25 x 25 mm. Stage position is feedback-controlled in X, Y, and Z to ~1 nm. Template leveling is controlled at three points to ~1 nm. Alignment and gap are detected simultaneously with a set of three ISPI microscopes. Both imprint systems reside in micro-environment enclosures within a Class 10 cleanroom.

Exploration of synergy between imprint lithography and Zone-Plate-Array Lithography (ZPAL), Interferometric Lithography (IL), Spatial-Phase-Locked E-Beam Lithography (SPLEBL), and other types of nanolithography unique to the NSL are underway. In an example of such synergy, the high-throughput, parallel-write capabilities of ZPAL are being used to streamline patterning of imprint templates. In another example, imprint lithography is being used to inexpensively transfer IL-patterned fiducial grids onto substrates, a step that may be essential to successful commercialization of SPLEBL. In yet another example (illustrated in a subsequent section), we use imprint lithography to fabricate arrays of zone plates.

We plan to employ imprint lithography systems for fabrication of coupled Josephson junction quantum bits for use in quantum computing.



Figure 1: A custom-designed imprint lithography system used with Interferometric-Spatial-Phase Imaging (ISPI) alignment and gap control. Three ISPI microscopes provide continuous position measurements for six-axis positioning ($X, Y, Z, \theta_x, \theta_y, \theta_z$) with sub-1 nm precision.

5. Imprint Lithography with Multilevel Alignment Via Interferometric-Spatial-Phase Imaging

Sponsors

Internal funds

Project Staff

Dr. Euclid E. Moon, Prof. Henry I. Smith

A critical requirement for widespread industrial utilization of imprint lithography is multilevel overlay capability. In journal articles [1, 2] we described a position metrology scheme, called Interferometric-Spatial-Phase Imaging (ISPI), which encodes alignment in the spatial phase disparity of complementary interference fringes, observed with oblique-incidence, long-working-distance, darkfield optical microscopes. We have applied ISPI to step-and-flash imprint lithography (S-FIL), in which alignment is actively measured and corrected with imprint fluid filling the template-substrate gap.

In previous S-FIL work, alignment marks were placed entirely outside of the imprinted area. However, it is highly desirable to detect alignment within the imprinted region, which implies use of a shallow phase grating as the alignment mark, and raises the issue of ISPI fringe contrast. Fringe contrast with a fused silica phase grating in an imprint fluid is 12% of the fringe contrast with air in the template-substrate gap, as predicted by two-dimensional finite-difference time-domain (FDTD) simulations, and confirmed by experiment. Despite the low fringe contrast,

experimental data (Figure 1) shows that ISPI can achieve *sub-nanometer* alignment detectivity under such conditions, the most stringent typically encountered in imprint lithography.

Figure 2 illustrates dynamic alignment control throughout the S-FIL imprint process. The data shows an initial condition in which ISPI controls alignment to <1 nm. In this particular example, alignment is disturbed by a mechanical impulse from opening of the UV shutter, but such disturbances, which would usually pass unnoticed, can be observed and corrected by ISPI. We believe these experiments, among others, indicate that ISPI is uniquely suited for application to S-FIL and other forms of imprint lithography. Commercial S-FIL imprint lithography tools now incorporate ISPI alignment technology, and have demonstrated overlay of $3\sigma = 7$ nm.

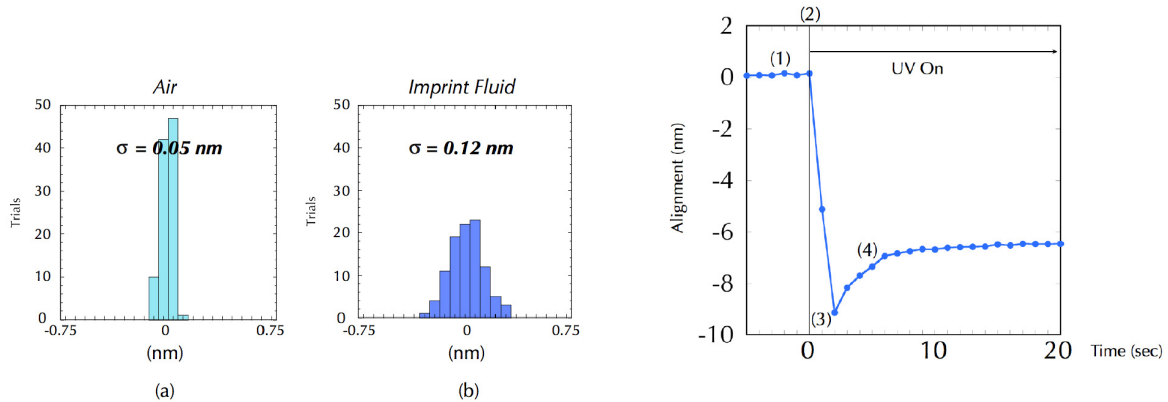


Figure 1: Alignment detectivity of ISPI with (a) air in the template-substrate gap ($\sigma = 0.05$ nm), and (b) imprint fluid in the gap ($\sigma = 0.12$ nm). Detectivity is reduced in the stringent case of phase gratings on the template, used with an imprint fluid of similar index of refraction, but remains within the sub-nanometer range. The template-substrate gap was mechanically locked during the experiment.

Figure 2: Plot of ISPI alignment data (1) before exposure, (2) at the instant the shutter to the UV lamp opens, (3) during misalignment caused by a mechanical shock transmitted from the UV lamp to the template, and (4) during correction of misalignment, until crosslinking solidifies the imprint fluid. The experiment demonstrates the ability of ISPI to detect and identify sources of misalignment on the nanometer level, as well as a limited ability to re-align during crosslinking of the imprint material. Improvements are readily achievable with increased feedback bandwidth.

References

- [1] E. E. Moon, L. Chen, P. N. Everett, M. K. Mondol, and H. I. Smith, "Interferometric-spatial-phase imaging for six-axis mask control," *J. Vac. Sci. Technol. B* **21**, 3112 (2003).
- [2] E. E. Moon, M. K. Mondol, P. N. Everett, and H. I. Smith, "Dynamic alignment control for fluid-immersion lithographies using interferometric-spatial-phase imaging," *J. Vac. Sci. Technol. B* **23**, 2607 (2005).

6. Absorbance-Modulation Optical Lithography

Sponsors

DRAPA

Project Staff

Dr. Rajesh Menon, Prof. Henry I. Smith

We are investigating absorbance modulation as a means to overcome the diffraction limit in far-field, optical-projection imaging. A substrate is coated with an absorbance-modulation layer (AML) in which illumination at one wavelength, λ_2 , renders the AML opaque, while illumination at a shorter wavelength, λ_1 , renders it transparent. When illuminated with a ring-shaped spot at λ_2 co-incident with a focused spot at λ_1 , the dynamic competition results in a nanoscale aperture, through which λ_1 can penetrate to the substrate beneath (see Fig. 1). The size of the aperture is limited only by the photokinetic parameters of the AML, and the intensities of the illuminations [1].

If the AML is placed atop a photoresist that is sensitive to λ_1 but not to λ_2 , patterns of arbitrary geometry can be written by scanning the substrate. The writing speed can be increased by using a large number of independently illuminated lenses operating in parallel, and scanning the stage [2]. This technology, which we call Absorbance-Modulation Optical Lithography (AMOL), will be maskless, fast, nanoscale and low-cost. AMOL resolution is determined by the ratio of the intensities at the two wavelengths. By simply scaling this ratio, it is possible to scale the transmitted spot far beyond the diffraction limit, enabling AMOL to eventually replace scanning-electron-beam lithography.

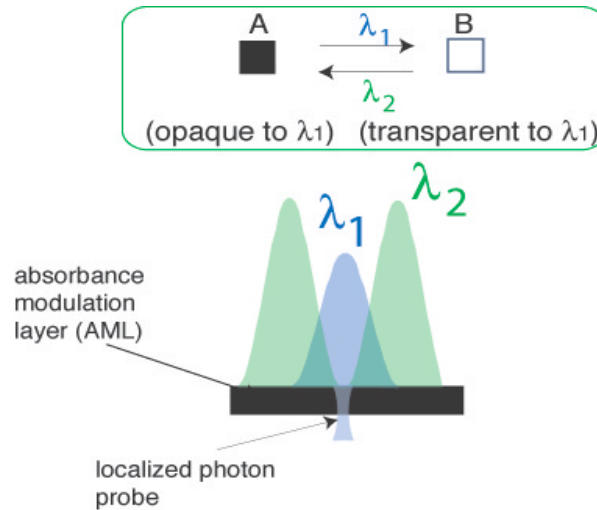


Figure 1: Absorbance modulation. The absorbance modulation layer can be made transparent or opaque depending upon the wavelength of illumination. By illuminating with both wavelengths at appropriate intensities, a stable, transparent aperture of nanoscale dimensions can be generated as shown.

References

- [1] R. Menon and H. I. Smith, "Absorbance modulation optical lithography," *J. Opt. Soc. Amer. A*, 23, 2290 (2006); R. Menon, H-Y Tsai and S. W. Thomas III, "Far-field generation of localized light fields using absorbance modulation," *Phys. Rev. Lett.* 98, 043905 (2007).

- [2] H. I. Smith, R. Menon, A. Patel, D. Chao, M. Walsh, G. Barbastathis, "Zone-plate-array lithography: a low-cost complement or competitor to scanning-electron-beam lithography," *Microelectron. Eng.*, 83, 956 (2006).

7. Replication of Diffractive-Optical Arrays Via Imprint Lithography

Sponsors

Internal funds

Project Staff

Dr. E. E. Moon, M. D. Galus, Dr. R. Menon, Prof. H. I. Smith

Diffractive-optical arrays serve important functions in a variety of applications, including zone-plate-array maskless lithography, in which they focus light to diffraction-limited spots and expose multiple features in parallel. Diffractive arrays are typically fabricated by e-beam lithography, but this is very time consuming and prone to defects. We investigated the feasibility of replicating such arrays using a custom step-and-flash imprint lithography (S-FIL) tool [1].

Imprint template patterns were fabricated as relief structures in bulk fused silica, using nickel liftoff after e-beam exposure of PMMA. The nickel pattern was used as a hardmask to dry etch the patterns into the underlying fused silica. After coating the template with a release layer, droplets of a low-viscosity imprint fluid were applied to the substrate surface, and the template was leveled and brought to within ~100 nm of the substrate. At that point the imprint fluid filled the template features via capillary action. The imprint fluid was crosslinked under UV exposure, and the template removed. The imprint process was completed in under 5 min. A two-step dry etch transferred the patterns into a transparent substrate. Figure 1 shows micrographs of the resulting imprinted and etched features [2].

The focusing capability of the imprinted diffractive elements was characterized by exposing single-spot features and comparing the feature width, or the derived point-spread function, with a finite-difference time-domain (FDTD) model, as illustrated in Fig. 2. We believe these experiments establish the efficacy of imprint lithography for reproduction of diffractive-optical arrays.

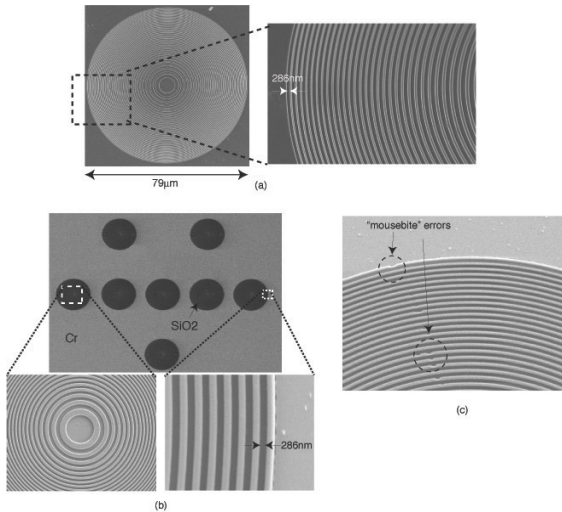


Figure 1: Scanning-electron micrographs of a zone plate imprinted in a fused silica substrate. (a) Imprinted pattern. (b) Etched pattern in fused silica. (c) Close-up view of etched patterns, indicating few local defects (“mousebites”). Moiré artefacts in the micrographs are generated by beating between the scan period of the SEM beam and the spatial periods of the zone plate.

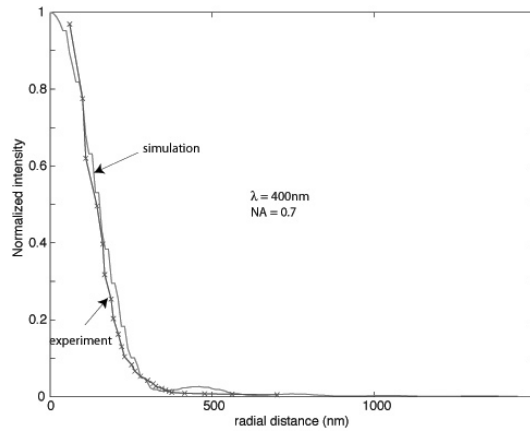


Figure 2: Point-spread function (PSF) characterization of the etched zone plates via single-spot exposures at increasing doses. After scaling, inverse diameters were plotted as a function of the dose. The FDTD-simulated PSF is also plotted for comparison. The parameters were $\lambda = 400 \text{ nm}$, $\text{NA} = 0.7$, $f = 40 \text{ mm}$. The data indicate the ability to achieve sub-wavelength focusing using imprinted zone plates.

References

- [1] E.E. Moon, M.K. Mondol, P.N. Everett, and H.I. Smith, “Dynamic alignment control for fluid-immersion lithographies using interferometric-spatial-phase imaging,” *J. Vac. Sci. Technol. B* **23**, p. 2607 (2005).
- [2] M.D. Galus, E.E. Moon, H.I. Smith, and R. Menon, “Replication of diffractive-optical arrays via photocurable nanoimprint lithography,” *J. Vac. Sci. Technol. B* **24**, p. 2960 (2006).

8. Interference Lithography

Sponsors

Singapore-MIT Alliance and internal funds

Project Staff

Thomas B. O'Reilly, Dr. Timothy Savas, Professor Henry I. Smith

The NanoStructures Laboratory has conducted research on interference lithography (IL) for many years, developing tools and techniques to create periodic structures (such as gratings and grids) over a wide range of spatial periods. The lab currently operates three IL systems. Two of them, the Lloyd’s mirror and Mach-Zehnder IL systems use 325 nm light from helium-cadmium lasers. The Lloyd’s mirror IL system can be quickly and easily configured to produce gratings with periods as small as 165 nm or as large as many microns. The flexibility and ease of use of this system enables its use by a large number of researchers to produce periodic and quasiperiodic structures for use in a wide range of research programs. The Mach-Zehnder IL system, while less flexible than the Lloyd’s mirror, produces higher quality gratings that are suitable for metrological applications. The third system, the Achromatic IL system (AIL) is a grating-based interferometer that writes 100 nm-period gratings using 193 nm light from an ArF excimer laser.

In addition, the NSL has close ties to the Space Nanotechnology Lab at MIT, which operates the NanoRuler. The NanoRuler is the most precise IL systems in the world.

We are currently developing a method to characterize photoresist performance by double-exposing a sample on an IL system; the sample is rotated slightly between the two exposures. By analyzing the resulting pattern one can determine how linewidth varies with exposure dose and dose modulation in fewer exposures than are required by previously described methods. The new method is currently being extended to make it possible to model variation of linewidth across the exposure area in systems such as the Lloyd's mirror or Mach-Zehnder IL systems.

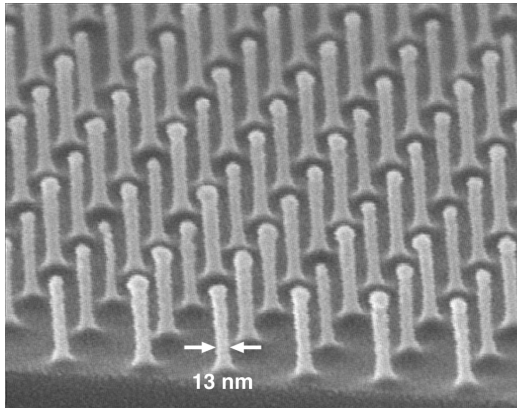


Figure 1: Scanning electron micrograph of a 100 nm-period grid produced with the AIL system. PMMA was exposed on top of an antireflection coating and the pattern was transferred into Si by reactive ion etching.

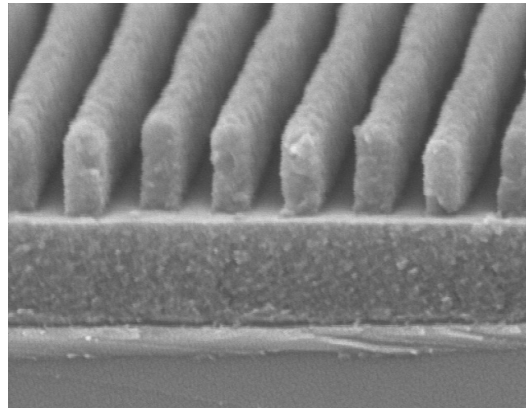


Figure 2: Micrograph of 165 nm period grating produced with the Lloyd's mirror in photoresist above an antireflection coating. The Lloyd's mirror system can be used to produce patterns with spatial periods ranging from 165 nm up to several microns.

References

- [1] Thomas B. O'Reilly and Henry I. Smith, "Photoresist characterization using double exposures with interference lithography," *J. Vac. Sci. Technol. B*, 26(1), 128-131 (2008).
- [2] Thomas B. O'Reilly and Henry I. Smith, "Linewidth Uniformity in Lloyd's Mirror Interference Lithography Systems", submitted to *J. Vac. Sci. Technol. B*

9. Immersion-Achromatic-Interference Lithography for Sub-100 nm-Period Structures

Sponsors

Singapore-MIT Alliance, Lincoln Laboratory, and internal funds

Project Staff

Thomas B. O'Reilly, Professor Henry I. Smith

Interference lithography (IL) is a means of using the coherent interference of light to produce periodic patterns. The spatial period, P , produced is dependent on the interference angle θ , wavelength of light, λ , and the refractive index of the incident medium, n , and is given by: $P = \lambda / 2n \sin(\theta)$. Reducing the period of the pattern is most commonly accomplished by reducing λ or increasing θ . As the interference angle cannot exceed 90° , and the selection of suitable short-wavelength sources is limited, reduction of P below $\lambda/2$ requires the use of an immersion fluid to reduce the effective wavelength of the light.

We are presently developing an immersion achromatic interference lithography system to extend our capability to produce fine-period patterns. The system being developed is similar to the lab's existing achromatic IL system, which produces 100 nm-period gratings, in that the new immersion system will use diffraction gratings to split and recombine 193 nm light from an ArF excimer laser. The addition of an immersion fluid, initially water, will allow the system to write patterns with periods of 70 nm. Use of higher index fluids will make it possible to write even finer patterns. Development of fabrication processes for the gratings is currently underway.

Gratings and grids produced with this tool will likely find applications similar to those produced by the existing AIL system, which includes templates for self assembly and gratings for atom-interferometry. The system could also be used to test materials including photoresists and immersion fluids at periods smaller than are possible with other lithography systems.

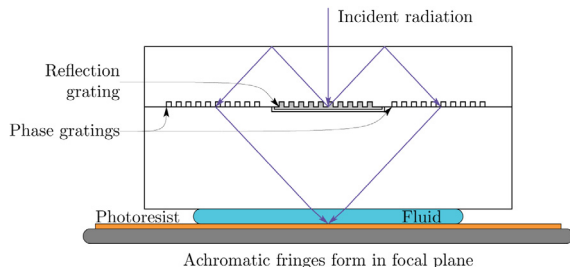


Figure 1: Schematic diagram of immersion achromatic IL system under development. Light from an excimer laser enters vertically at the top of the interferometer and is diffracted by a reflection grating. The light reflects off the top of the interferometer where a pair of transmission gratings diffract the light back toward the focal plane where it exposes a photosensitive substrate.

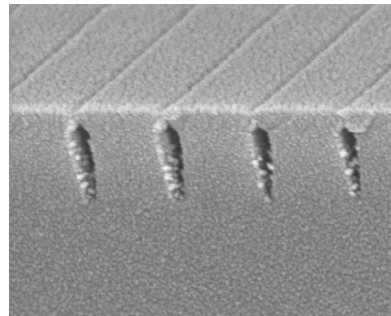


Figure 2: Transmission grating fabricated in glass with a period of 266 nm. The geometry of the grating must be carefully controlled to get reasonable diffraction efficiency into the desired orders, which presents a fabrication challenge.

10. Sub-Nanometer Accuracy in Lateral Tip-to-Substrate Positioning for Scanning-Probe Lithography

Sponsors

Internal Funding

Project Staff

Dr. Euclid E. Moon, Prof. Karl Berggren, Prof. Henry I. Smith

In scanning-probe microscopy or lithography, a longstanding problem is that the lateral position of the tip relative to the substrate is subject to perturbations due to thermal expansion and other distortions in their long mechanical connection. Shortening the mechanical path to improve tip registration would limit a scanning probe to small substrates. Stiffening the mechanical connection has limited effectiveness. In either case, the tip-to-substrate position is unknown until scans are performed, and, as a result of the finite time required to complete a scan, mechanical distortions of tip-to-substrate position typically are evident between the completion of the scan and the subsequent positioning of the tip.

In this work we apply an interferometric position metrology technique, called Interferometric-Spatial-Phase Imaging (ISPI), to directly and continuously measure and control lateral tip-to-substrate position in a scanning-probe system, and demonstrate use of tip-to-substrate control for nanometer-precision lithography.

Simple modifications were made to adapt ISPI to a commercially available AFM (Veeco Dimension 3000), as shown in Fig. 1. Modifications include the addition of two ISPI microscopes, a super-invar tip holder with a fused-silica reference flat containing ISPI marks, and a closed-loop piezo stage with internal capacitive sensors under the substrate. Observing displacement with ISPI yields previously unattainable insight into the behavior of the tip relative to the substrate. Figure 2 illustrates tip-to-substrate behavior while attempting to hold the tip at a single point using (a) the open-loop piezo, (b) the closed-loop piezo, and (c) ISPI feedback to the substrate piezo stage to correct for unintended displacements. Figure 3 shows the ability to place the tip at a regular array of points, as well as repeatability, using each of the three tip positioning methods (a), (b), (c). Figure 4 shows statistics for tip positioning at a grid array using ISPI. Lithography performed in a polymer with a tapping tip is shown in Fig. 5, in which two identical closed-path figures are described by the tip under ISPI control, directly on top of each other. Attempts at writing similar patterns without using ISPI position control result in overlay errors of several tens, or hundreds, of nanometers. We believe these experiments, among others, demonstrate the benefits of direct, continuous monitoring and control of tip-to-substrate position for nanolithography, as well as metrologically-accurate scanning-probe imaging.

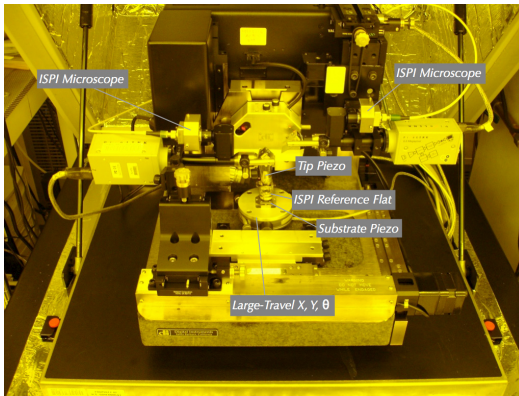


Figure 1: Photograph of the ISPI-modified AFM. The additional ISPI hardware consists of microscopes for measuring X and Y position, and a custom super-invar tip holder with ISPI marks. A closed-loop piezo stage replaces the substrate chuck.

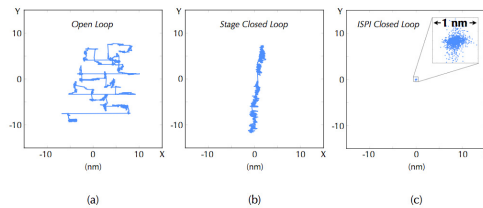


Figure 2: ISPI measurements of tip-to-substrate position while attempting to hold the tip at a single point over the substrate using (a) an open-loop piezo, (b) a closed-loop piezo stage, and (c) ISPI to feedback-control tip-to-substrate position. Although both open-loop and closed-loop piezo stages permit drift of more than 10 nm during 10 minutes, ISPI measurements indicate elimination of tip-to-substrate drift within $3\sigma = 0.3$ nm in X and $3\sigma = 0.4$ nm in Y.

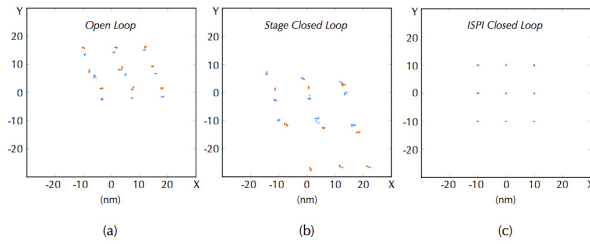


Figure 3: ISPI measurements of attempts to position a tip on a 3x3 grid, with 10 nm period. Data were taken using the (a) open-loop piezo; (b) closed-loop piezo; and (c) ISPI feedback control. In each case the tip was held at an intended position for 2 minutes, and then moved to the next point, following a serpentine scan, starting at the lower left point. The grid scan was repeated in the reverse order, as shown by a second set of points that are intended to overlay upon the first set. Errors amount to several nanometers, or tens of nanometers, with either open-loop or stage closed-loop operation. Data using ISPI control for the two grid scans are overlaid, and are indistinguishable, as shown in (c).

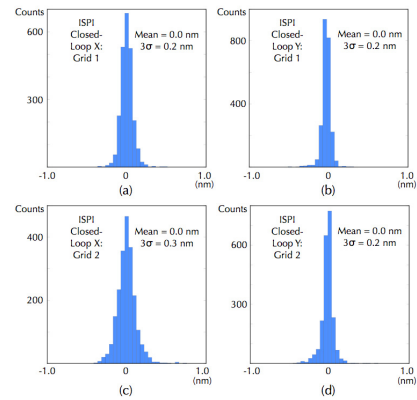


Figure 4: Plots of the disparity of ISPI positioning from the intended pattern placement, taken during position locking of the tip in the two successive grid scans shown in Fig. 3(c). (a), (b) ISPI control results in positioning at grid points with overlay disparities of $3\sigma = 0.2$ nm in X and $3\sigma = 0.2$ nm in Y. In the second grid scan (c), (d), the deviation from the desired positions was $3\sigma = 0.3$ nm in X and $3\sigma = 0.2$ nm in Y. The data show good placement accuracy within each grid scan, as well as good repeatability between successive scans. The mean position deviation was 0.0 nm in each scan.

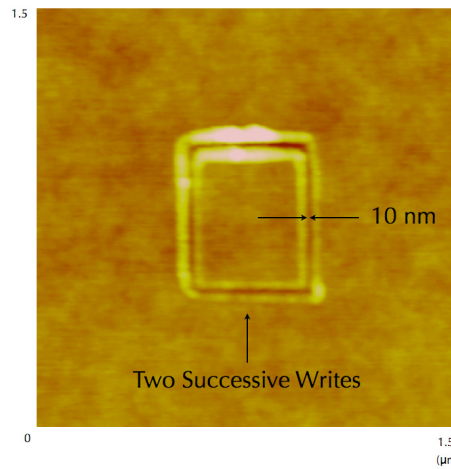


Figure 5: AFM scan of patterns written in PMMA showing overlay of two patterns using ISPI control. The double-patterned scan employing ISPI is indistinguishable from a single-patterned scan, indicating an upper bound on the overlay (<10 nm) that is limited by the lateral detectivity of the AFM (256x256 data points in a 1.5x1.5 μm scan).

References

- [1] Euclid E. Moon and Henry I. Smith, "Nanometer-precision pattern registration for scanning-probe lithographies using interferometric-spatial-phase imaging," *J. Vac. Sci. Technol. B* **24**, 3083 (2006).
- [2] Euclid E. Moon, Jan Kupec, Mark K. Mondol, Henry I. Smith, and Karl K. Berggren, "Atomic-force lithography with interferometric tip-to-substrate position metrology," Submitted for Publication, *J. Vac. Sci. Technol. B* **25** (2007).

11. Sub-10 nm Feature Resolution in Arbitrary Pattern Geometries Using Atomic-Force Lithography

Sponsors

Internal Funding

Project Staff

Dr. Euclid E. Moon, Prof. Henry I. Smith

Research in imprint lithography has demonstrated successful pattern transfer of 2 nm features from imprint templates to substrates. An open issue is imprint template fabrication at this resolution. Electron-beam lithography may be extendable to the sub-10 nm domain, however, limitations exist due to electron scattering and proximity effects. Helium-ion lithography can reach a theoretical resolution of ~1 nm, although this potential has yet to be demonstrated, and pattern registration at the sub-1 nm level remains an obstacle.

In this work we demonstrate a simple method of using a scanning probe tip to write sub-10 nm features [1] in a polymer, such as PMMA, on an imprint template.

We employ a tip with an additional self-assembled spike of carbon or tungsten. Tips are shown in Fig. 1 to be capable of resolving adjacent C₆₀ molecules, indicating the tip diameter is <0.7 nm. Deconvolution of the tip shape with the known geometry of C₆₀ molecules suggests a tip diameter of 0.28 nm, or approximately 3 carbon atoms.

During lithography, the tip is operated in tapping mode, albeit closer to the surface than in the conventional imaging mode. Figure 2 illustrates 10 nm half-pitch gratings written with the tip. Figures 3 and 4 show arbitrary patterns written with the tip, having FWHM linewidths of 9.3 nm and 2.9 nm, respectively. We will utilize sub-nanometer diameter tips with interferometric tip-to-substrate control, for sub-nanometer lateral positioning, as well as continuous interferometric tracking of tip height, a necessary factor for consistent linewidth control.

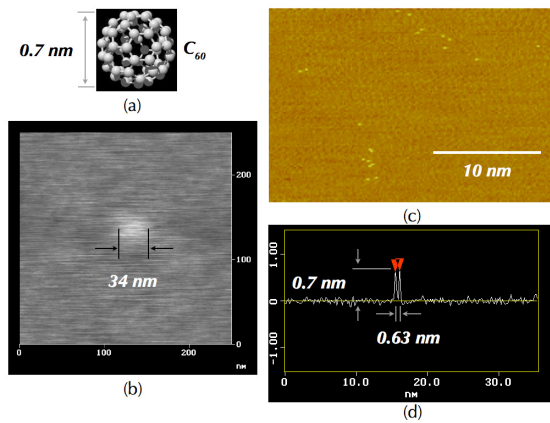


Figure 1: (a) Model of a C_{60} molecule. (b) AFM scan of a single fullerene (C_{60}) molecule using a conventional etched silicon tip. Convolution of the tip diameter with the molecule produces a 34 nm smear. (c) AFM scan of fullerene (C_{60}) molecules using a diamond-like carbon spike tip, demonstrating resolution of individual molecules. (d) Cross-section of a pair of fullerenes within Fig. 1(c), indicating the carbon tip diameter is less than the intermolecular distance (<0.7 nm).

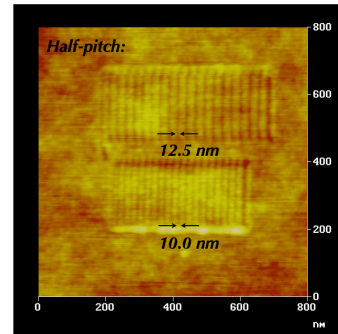


Figure 2: AFM scan of gratings written with a tungsten tip in PMMA. Grating half-pitch is 12.5 nm and 10.0 nm in the upper and lower gratings, respectively.

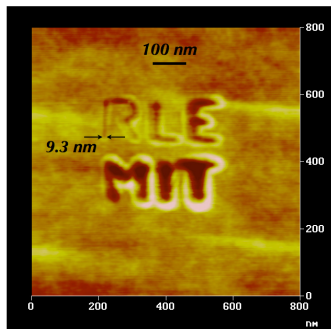


Figure 3: AFM scan of an arbitrary pattern written with a tungsten tip in PMMA on a fused silica imprint template. Measured FWHM linewidth is 9.3 nm. The residual substrate tilt and surface topography varied the linewidth during the lithography.

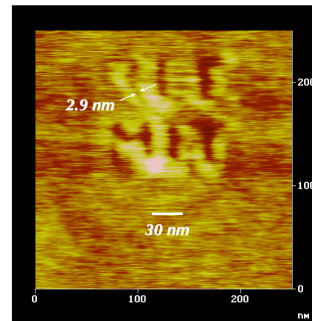


Figure 4: AFM scan of an arbitrary pattern written with a carbon tip in PMMA. Measured FWHM linewidth is 2.9 nm.

References

- [1] Euclid E. Moon and Henry I. Smith, “Nanometer-precision pattern registration for scanning-probe lithographies using interferometric-spatial-phase imaging,” *J. Vac. Sci. Technol. B* **24**, 3083 (2006).

12. Building Three-dimensional Nanostructures via Membrane Folding

Sponsors

Institute for Soldier Nanotechnologies, NSF Graduate Research Fellowships

Project Staff

William .J. Arora, Anthony .J. Nichol, Professor George. Barbastathis, Professor Henry .I. Smith

In Nanostructured Origami¹ thin membranes are patterned in 2D and are then automatically folded in sequence to produce a 3D configuration. We have developed methods of both folding actuation and folded-structure alignment for patterned silicon-nitride membranes. We have demonstrated that ion implantation can be used to fold membranes. Figure 1 shows data from membranes implanted with high doses of helium. The implanted ions create stress, forcing the membrane to bend. A minimum bend radius of 1 μm using 100 nm-thick silicon nitride was achieved. The resulting 3D structure remains folded unless heated above 400C, at which point the helium diffuses out and the structure unfolds. In addition to experimental demonstration, we model the physics of the ion implantation to show that the ion-implant profile correlates to the observed folding. This is most clearly evidenced by the fact that membranes given low energy (shallow depth) implants fold downwards while membranes given high energy (large depth) implants fold upwards. Magnetic forces are an alternate actuation method to fold, and to align and reconfigure nanopatterned membranes.² After folding, the membranes accurately self-align when brought into close proximity due to the interactive magnetic force between the arrays of nanomagnets. Since the self-alignment accuracy is better than the lithographic resolution, the membranes may be self-aligned to nanometer precision. We are also developing a nanomagnetic stepper that utilizes the force between arrays of nanomagnets to precisely move a nanopatterned membrane along a substrate. After folding and magnetically aligning two membranes, the system is actuated by an external magnetic field that rotates or flips the magnetization of the nanomagnets, thus changing the equilibrium position. Figure 2a shows a micromagnetic simulation of a bi-stable switcher that changes between two positions by rotating the external field. Figure 2b shows a schematic of the nanomagnet stepper, which uses circular nanomagnets that shift one step per full rotation of the external magnetic field. The stepper is wirelessly controlled and is non-hysteretic so the need for feedback is eliminated. We are exploring the stepper's use for reconfigurable photonic systems and wireless nano-device control.

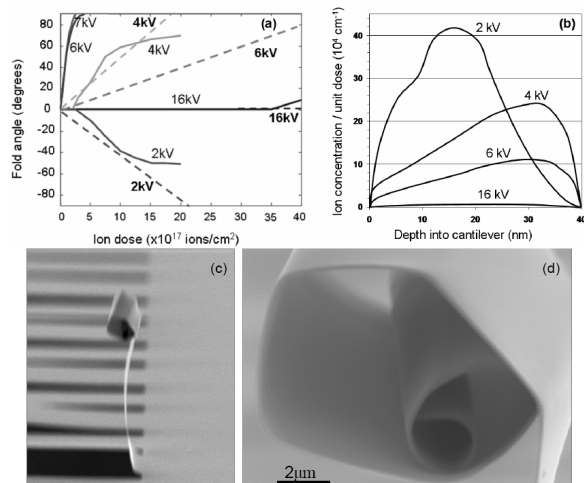


Figure 1. a) Fold angle vs dose for different 40 nm thick silicon nitride cantilevers implanted with helium (solid lines are experimental; dashed lines are prediction) b) Corresponding ion profiles within the cantilever. c, d) Experimental demonstration of folding.

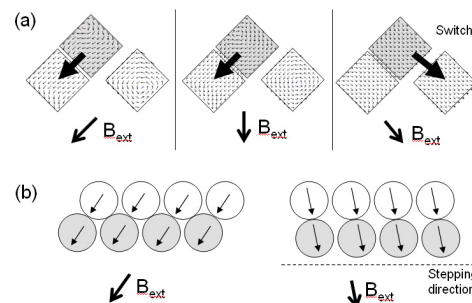


Figure 2. (a) Micromagnetic model of a nanomagnetic switcher and (b) schematic of a nanomagnet stepper motor that moves one period with each full rotation of the external magnetic field.

References

- [1] H.J. In, W.J. Arora, T Buchner, S.M. Jurga, H.I. Smith, G. Barbastathis. *2004 4th IEEE Conference on Nanotechnology (IEEE Cat. No.04TH8757)*, 2004, p 358-60 JVSTB:
- [2] A.J. Nichol, Paul S. Stellman, W.J. Arora, George Barbastathis. *"Two-step magnetic self-alignment of folded membranes for 3D nanomanufacturing."* Accepted: *J. Microelectronics Engineering* Dec. 2006.

13. Localized Substrate-Removal Technique Enabling Optical Intrachip Communication in Bulk-Silicon CMOS

Sponsors

DARPA

Project Staff

Charles. W. Holzwarth, Jason S. Orcutt, Jie Sun, Hanqing Li, Milos A. Popovic, Vladimir Stojanovic, Judy L. Hoyt, Rajeev J. Ram, and Henry I. Smith

Efforts elsewhere to integrate photonics with CMOS electronics require customization of the fabrication process to provide low-loss in the photonic components [1]. This compromises electronic performance, throughput, and cost. Customizations included thick low-index cladding layers, silicon-on-insulator material and electron-beam lithography. While tolerable for some applications, such customization is considered unacceptable for microprocessors and DRAM, circuits that would benefit the most from optical intrachip communication. In order to integrate photonics with circuits produced in high volume, one must be able to work within the constraints of commercial bulk CMOS process flows by utilizing industry-standard material layers, thicknesses, processing steps and tools. Waveguides fabricated out of the polysilicon layer used for transistor gates and poly-resistors above the shallow-trench isolation (STI) layer would have a propagation loss of the order of 1000 dB/cm since the STI layer (<400 nm) is not thick enough to prevent the guided optical mode from "leaking" into the high-index Si substrate.

To overcome this problem, we have developed a novel post-processing technique using XeF₂ to locally remove the silicon underneath the STI layer, as shown in Fig. 1. The creation of air tunnels under the polysilicon waveguides eliminates propagation loss due to leakage into the substrate, and minimizes impact on the electrical, thermal, and mechanical performance of the electronics. XeF₂ gas is used because it etches Si isotropically, can undercut large areas without stiction problems, and has a high silicon-to-oxide etch-rate selectivity (>1000:1). We have used this method to fabricate waveguides in polysilicon-on-oxide films (Figure 2). The propagation loss of these waveguides was measured to be ~10 dB/cm at 1550 nm. Most of this loss is attributed to material absorption and scattering from surface and sidewall roughness [2].

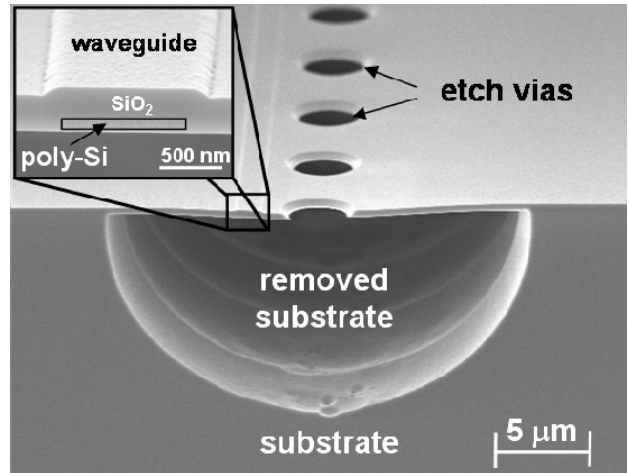
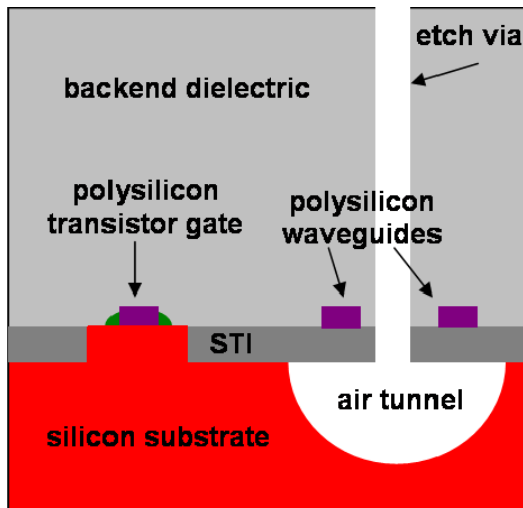


Figure 1: Sketch of the cross-section of a bulk CMOS chip showing how electronics and photonic devices can be fabricated on the same chip with only the addition of a post-processing step to locally remove the silicon substrate beneath the polysilicon waveguides.

Figure 2: Scanning-electron micrograph of fabricated poly-silicon waveguide using the XeF₂ based substrate removal technique. The inset shows a close-up of the waveguide. The SiO₂ cladding beneath the poly-silicon is only 50 nm thick resulting in loss >1000 dB/cm before the localized substrate removal step. After removal, the loss is reduced to approximately 10 dB/cm.

References

- [1] J.S. Orcutt *et al.*, "Demonstration of the first electronic photonic integrated circuit in a commercial scale bulk CMOS Process," Submitted to the Conference of Lasers and Electro-Optics (CLEO), San Jose, California, May 5-9, 2008.
- [2] C.W. Holzwarth *et al.*, "Localized Substrate Removal Technique Enabling Strong-Confinement Microphotronics in Bulk-Si CMOS Processes," Submitted to the Conference of Lasers and Electro-Optics (CLEO), San Jose, California, May 5-9, 2008.

14. Nanofabrication of Optical Microring Filter Banks for Ultra-Fast Analog-to-Digital Converters

Sponsors
DARPA

Project Staff

Charles W. Holzwarth, Tymon Barwicz, Milos A. Popović, Anatoly Khilo, Marcus Dahlem, Erich P. Ippen, Franz X. Kärtner and Henry I. Smith

Progress in designs and nanofabrication techniques for microring-resonators in high-index-contrast materials have made possible the wide spectral spacing between resonances and low loss required for electronic-photonic integrated circuits including ultra-fast analog-to-digital converters [1]. Achieving accurate resonant-frequency spacing of microring-filters is critical for these devices. In the NanoStructures Laboratory we have developed a technique using scanning-electron-beam lithography (SEBL) that is capable of accurately controlling the resonant

frequency spacing in microring-resonator filter banks. The resonant wavelength of a microring-resonator filter is dependant on both the ring radius and the effective index of refraction of the ring waveguide. The effective index is controlled lithographically by controlling the width of the ring waveguide. Although it is simple to change both the width and the radius of the ring in the SEBL layout, this is limited to discrete jumps corresponding to the step size of the SEBL system. In order to have 1 GHz control of the resonant frequency for the designed filters the SEBL systems would need a step size of 30 pm. In our process this limitation of discrete step size is overcome by modulating the electron beam dose to precisely control the width of the ring waveguide [2].

In our experiment second-order microring-resonator filters, fabricated in silicon-rich silicon nitride and overclad with HSQ, were used in a microring filter banks (Figure 1a, 1b). Using dose modulation, twenty-channel dual-filter banks with a target channel spacing of 80 GHz were fabricated and tested, demonstrating control of changes in the average ring-waveguide width of 0.10 nm, despite the 6 nm SEBL step size (Figure 1c). Variations between filter responses were due to slight frequency mismatches between rings of the same filter, we demonstrated that this can be corrected by thermal trimming with integrated microheaters.

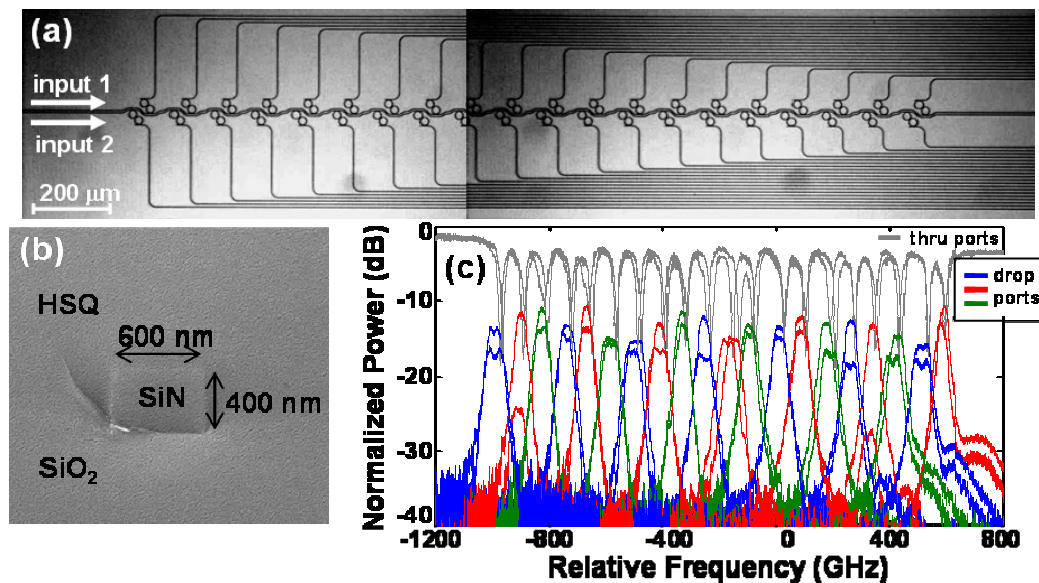


Figure 1: a) Scanning-electron micrograph of fabricated second-order twenty-channel dual-filter bank and b) cross-section of overclad waveguide. c) Filter response of second-order twenty-channel dual-filter bank with an average channel spacing of 83 GHz.

References

- [1] T. Barwicz, M.A. Popovic, P.T. Rakich, M.R. Watts, H.A. Haus, E.P. Ippen, H.I. Smith, "Microring-resonator-based add-drop filters in SiN: fabrication and analysis," *Optics Express* 12(7): (2004).
- [2] C.W. Holzwarth, T. Barwicz, M. A. Popović, P. T. Rakich, F. X. Kaertner, E. P. Ippen, and H. I. Smith, "Resonance-frequency control of high-index-contrast microphotonic cavities at fabrication," *JVST B* 24(6): (2006).

15. Nanofabrication of Hitless Reconfigurable Optical Add-drop Multiplexers Based on Silicon Microrings

Sponsors

DARPA and internal funds

Project Staff

Charles W. Holzwarth, Tymon Barwicz, Milos A. Popovic, Peter T. Rakich, Marcus Dahlem, Fuwan Gan, Erich P. Ippen, Franz X. Kaertner, and Henry I. Smith

Reconfigurable optical add-drop multiplexers (ROADMs) are key components of modern optical networks. Data in optical fibers is carried at numerous wavelengths, each defining a specific “channel.” The ROADMs allow the rerouting (“dropping”) of a subset of the data channels traveling in an optical fiber, replacing these with new data streams (“adding”) at the previously rerouted wavelengths. The term “reconfigurable” indicates that the subset of dropped channels can be changed “on the fly,” i.e., while the ROADM is in operation. For a ROADM to be truly useful in an optical network it must be “hitless,” that is, it must enable tuning from one channel to a second channel without affecting the data transmitted on any of the other channels.

In our previous work, we developed precision nanofabrication techniques that enabled us to demonstrate the most advanced microring filters reported to date in silicon-rich silicon nitride [1,2]. In the present work, we employed silicon microrings to take advantage of their lower optical loss and higher thermo-optic coefficient, allowing wide tuning of the operating wavelengths of the ROADM via integrated heaters. Figure 1 presents a cross-sectional diagram and top-view micrograph of our implementation of a silicon waveguide and a hitless ROADM with integrated microheaters. Line-edge roughness is of critical concern in silicon waveguides as it translates into significant propagation loss via scattering of the guided mode. We found that the smoothest waveguides were obtained using hydrogen silsesquioxane (HSQ) as an e-beam resist and an etch-mask for the subsequent HBr-based reactive-ion etching. Figure 2 presents a scanning-electron micrograph of a coupling region between a microring and a bus waveguide defined in HSQ. The patterning is based on scanning-electron-beam lithography.

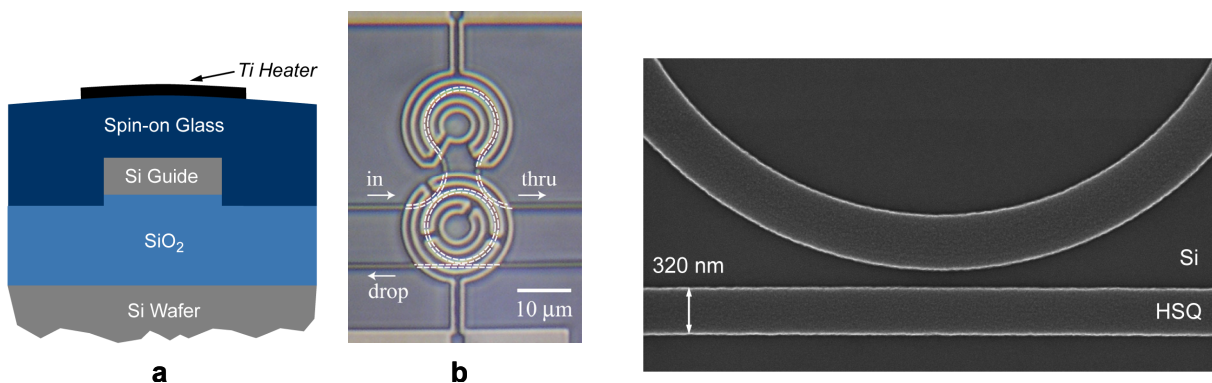


Figure 1: (a) Cross-sectional schematic of a silicon waveguide with an integrated titanium heater. Spin-on glass is used for the upper cladding of the waveguide to allow self-planarization and to avoid filling problems in narrow gaps. (b) Top-view optical micrograph of the silicon-microring hitless ROADM with titanium microheaters.

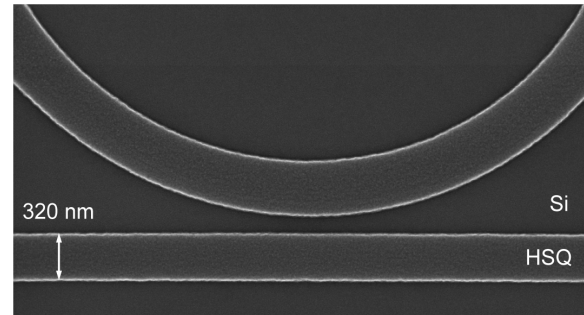


Figure 2: Top-view scanning-electron micrograph of a coupling region defined in HSQ. The patterning was done with scanning-electron-beam lithography. The minimum feature size required (e.g., the gap) is ~100 nm and must be controlled to ~5 nm.

References

- [1] M.A. Popović, T. Barwicz, M.R. Watts, P.T. Rakich, L. Socci, E.P. Ippen, F.X. Kärtner and H.I. Smith, "Multistage high-order microring-resonator add-drop filters," *Opt. Lett.*, 31(17): 2571-2573 (2006).
- [2] T. Barwicz, M.R. Watts, M.A. Popović, P.T. Rakich, L. Socci, F.X. Kärtner, E.P. Ippen and H.I. Smith, "Polarization-transparent microphotonic devices in the strong confinement limit," *Nature Photonics*, 1: 57-60 January (2007).

16. Microscopy Beyond the Diffraction Limit Using Absorbance Modulation

Sponsors

MIT Deshpande Center

Project Staff

Dr. Rajesh Menon, Hsin-Yu Tsai, Prof. Henry I. Smith

Absorbance Modulation Imaging (AMI) is an approach to overcome the optical diffraction limit in the far-field, thereby achieving macro-molecular resolution with photons. Preliminary experiments show promising results that agree well with theoretical predictions [1].

AMI relies on an absorbance-modulation layer (AML), composed of photochromic molecules. Illumination at one wavelength, λ_2 , renders the AML opaque, while illumination at a shorter wavelength, λ_1 , renders it transparent. When illuminated with a ring-shaped spot at λ_2 co-incident with a focused spot at λ_1 , the dynamic competition results in a nanoscale aperture, through which λ_1 can penetrate to the substrate beneath. The size of the aperture is limited only by the photo-kinetic parameters of the AML and the intensity ratio of the two illuminating wavelengths, not the absolute intensities [2]. By scanning this dynamic nanoscale aperture over the sample, resolution beyond the far-field diffraction limit is achieved. A related technique was demonstrated in stimulated-emission-depletion (STED) fluorescence microscopy [3]. However, while STED requires high power pulsed illumination and fluorescent markers, AMI can operate at low illumination intensity. A schematic of an AMI microscope is shown in Figure 1. Collimated beams at λ_1 and λ_2 illuminate the *dichromat*, a binary phase element, which creates a ring-shaped spot at λ_2 and a round spot at λ_1 . Figure 2 shows the phase transmission function of a dichromat and the intensity distributions in its focal plane for the two wavelengths.

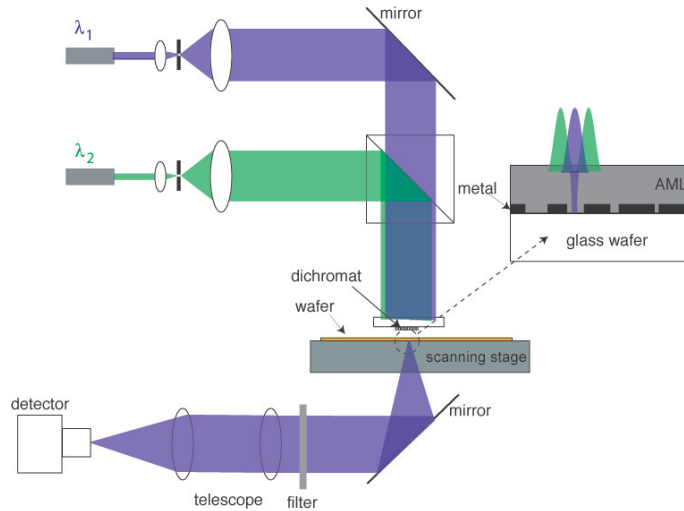


Figure 1: Schematic of absorbance-modulation imaging (AMI) microscope. The ring illumination at λ_2 creates a local subwavelength aperture for λ_1 in the AML through which the underlying object is illuminated and the scattered light collected. Multiple dichromats generate separate signals, enabling parallelism and enhanced throughput. The inset shows a schematic of a resolution test structure consisting of metal lines on a glass wafer.

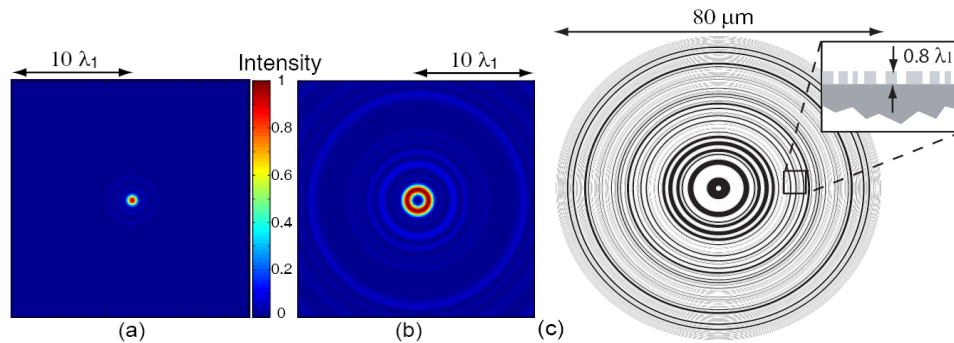


Figure 2: Output light intensity distributions at (a) λ_1 400nm, (b) λ_2 532nm, and (c) the phase transmission function of the dichromat. The phase step in this case is $0.8\lambda_1$ as shown in the inset of (c). The dichromat creates ring-shaped illumination for λ_2 and a focal spot for λ_1 .

References

- [1] R. Menon, H-Y Tsai, and S. W. Thomas III, "Far-field generation of localized light fields using absorbance modulation," *Phys. Rev. Lett.* 98(4): 043905 (2007).
- [2] R. Menon and H. I. Smith, "Absorbance modulation optical lithography," *J. Opt. Soc. Am. A* 23(9): 2290-2294 (2006).
- [3] S.W. Hell and J. Wichmann, "Breaking the diffraction resolution limit by stimulated emission: stimulated-emission-depletion fluorescence microscopy," *Optics Lett.* 19(11): 780-782 (1994).

17. Three-Dimensional Photonic Crystals in Si_3N_4 and Si by Assembly of Prepatterned Membranes

Sponsors

National Science Foundation and the Defense Threat Reduction Agency (DTRA)

Project Staff

Amil Patel, Corey Fucetola, Dr. Euclid E. Moon and Professor Henry I. Smith

The diffraction of light within periodic structures (so called “photonic crystals”) offers a wide variety of opportunities for controlling and manipulating light. Most research to date has focused on 2-dimensional (2D) photonic crystals, because highly developed planar-fabrication techniques (i.e., lithography followed by pattern transfer) are directly applicable. However, the full potential of photonic crystals in futuristic sensing, communication and computation systems is best achieved with 3-dimensional (3D) structures. The problem is that new methods of 3D fabrication need to be developed to achieve desired complex structures over large areas with low cost and high yield.

Interference lithography can produce periodic 3D structures in photosensitive polymers, but the introduction of deviations from perfect periodicity (i.e., waveguides and structures that constitute “devices” within the periodic matrix, so-called “defects”) is highly problematic. Moreover, it’s not clear that backfilling 3D polymeric structures is applicable to a suitable range of materials. Layer-by-layer methods the use scanning-electron-beam lithography enable the controlled introduction of defects, but such fabrication is generally tedious, slow, low yield, and covers impractically small areas (e.g., <0.1mm on edge).

We describe a novel approach in which the 3D photonic-crystal structure is fabricated by assembling membranes that are patterned in advance using conventional planar methods (Figure 1). This approach minimizes the yield problem because membranes can be inspected and selected before assembly, and the desired waveguides and devices, can be introduced at any level in the assembly. When brought into contact, membranes that are free of particulate and other contamination will bond spontaneously by van der Waals or other mechanisms.

Previously we reported using low-stress Si_3N_4 membranes as the test vehicle. 2D periodic structures were etched into free-standing membranes, and nonaligned stacking carried out (Figure 2). Currently, we are addressing the lithographic challenge of patterning a large-area photonic structure in conjunction with custom alignment marks that will assist in gap detection and lateral overlay. In addition, we are developing a process for creating 3D photonic crystals in Si, using coherent-diffraction lithography and HBr reactive-ion etching. The Si membranes are obtained from SOI wafers.

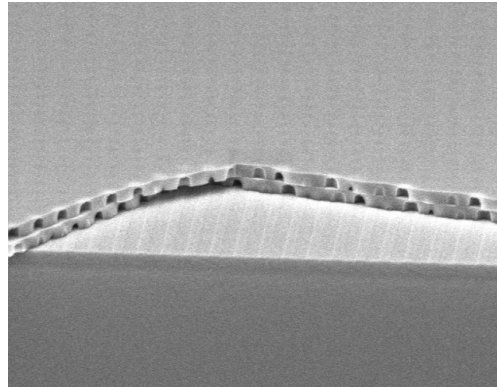
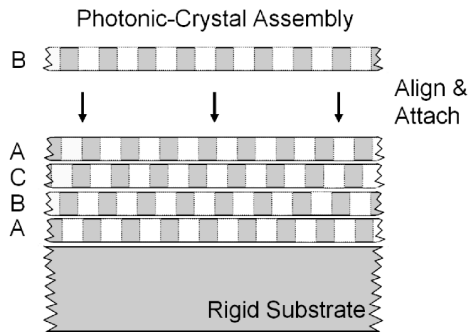


Figure 1: Depiction of the layer-by-layer stacking approach to 3D photonic crystal fabrication. All the layers in the photonic crystal are fabricated in parallel. This reduces processing cycles, which will help improve yield and reduce lead times.

Figure 2: Initial stacking experiment. A patterned SiN membrane is brought into contact with SiN substrate. The pitch of the array is 600nm and the membrane is 350nm thick. A second patterned membrane is brought into contact with the first.

References

- [1] A.A. Patel and H.I. Smith, "Membrane stacking; A new approach for three-dimensional nanostructure fabrication," *J. Vac. Sci. Technol.* **B 26**, 2662-2664 (2007).

18. Fabrication of Suspended Discs in Si₃N₄ Membranes for Observation of the Poisson Spot with Deuterium

Sponsors

Graz University of Technology (European Union FP6, program NEST - Adventure, contract nr. 509014, project INA) and internal funds.

Project Staff

Amil Patel, Thomas Reisinger (visiting student from Univ. Bergen, Norway), Professor Bodil Holst (Univ. Bergen, Norway) and Professor Henry I. Smith

The observation of a bright central spot in the shadow of an opaque circular object, the so-called Poisson Spot, was a historically important experiment establishing the wave nature of light. The same interference phenomenon should occur with material particles. To conduct an experiment to observe the Poisson Spot with monochromatic deuterium molecules D₂, we fabricated free-standing discs of silicon nitride, shown in Fig. 2.

The discs had a diameter of 60 μm and a thickness of 500 nm, centered within a 400 μm-diameter window and supported by four 3μm-wide support bars. The key parameters for the disc include thickness, ellipticity and edge roughness. Scanning-electron-beam lithography was used to pattern the area of the disc and the support bars on a Si₃N₄ membrane.. PMMA was used as the electron-beam resist, and the pattern was transferred to a chromium hardmask via a wet etch. The negative space was etched away using reactive ion etching. Figure 1 explains the configuration of the molecular beam experiment. Figure 2 shows a final device in Si₃N₄. Figure 3 shows the observation of the Poisson Spot through experiments run by our colleagues at the

Graz University of Technology. Experimental results match well with a model that accounts for disc edge corrugation and van der Waals interactions.

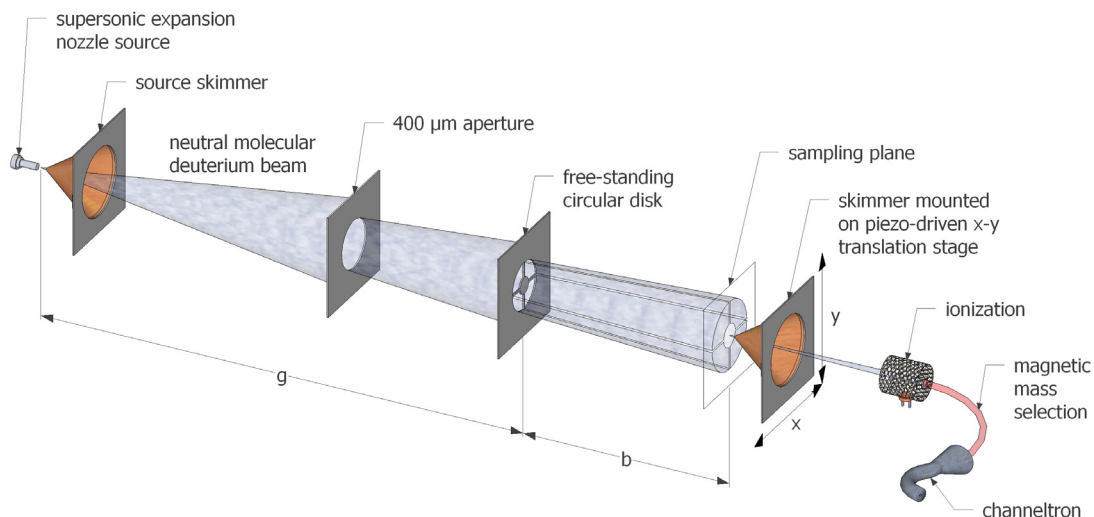


Figure 1: The schematic depicts the configuration of the molecular Poisson Spot experiment. The deuterium (D_2) beam is created in a supersonic expansion from a 10- μm nozzle. A source skimmer of 50 μm diameter is used to restrict the virtual source size to less than the diameter of the free-standing disc, which was 60 μm in the experiment. The geometrical shadow of the free-standing disc is stepped-across in the transversal plane using an 11- μm skimmer. The transmitted beam flux is recorded in an electron-bombardment detector.

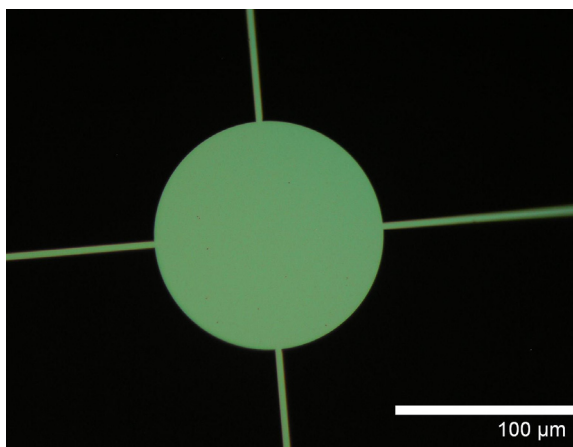


Figure 2: Optical micrograph of the most recently fabricated free-standing disc. (There is no material in the dark regions.) The disc obstruction is 100 μm in diameter and about 500nm thick. SEM metrology showed that edge roughness was under 50nm.

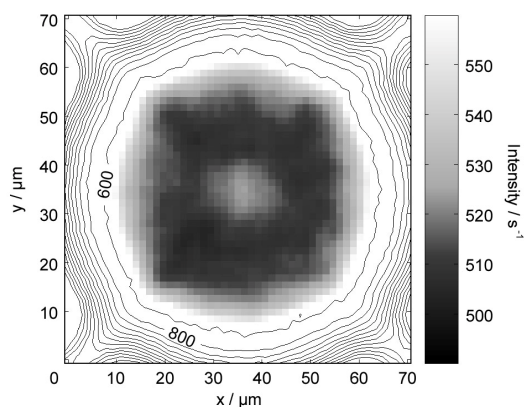


Figure 3: Deuterium Poisson Spot. Shown is the first Poisson Spot realized with molecules. The central part of the shadow is amplified as a grey image plot. The image is the sum of 24 images recorded consecutively at a sampling distance of 321 mm.

References

- [1] T. Reisinger, G. Bracco, S. Rehbein, S. Schmahl, W. E. Ernst, B. Holst, "Direct Images of the Virtual Source in a Supersonic Expansion," *J. Phys. Chem.* vol. A76, pp. 12620 – 12628 (2007).
- [2] T. Reisinger, A. Patel, H. Reingruber, K. Fladischer, W.E. Ernst, G. Bracco, H.I. Smith, B. Holst, "Poisson's Spot with Molecules," submitted to *Nature*.

19. Fabrication of Inverted-Pyramid Arrays in Si for Templated Self Assembly

Sponsors

Singapore-MIT Alliance

Project Staff

Dr. Timothy Savas, Thomas B. O'Reilly and Professor Henry I. Smith

In support of the Singapore-MIT Alliance, the lab's interference-lithography (IL) has been used to fabricate two types of patterned substrates for use in research on templated self-assembly.

The first set of substrates was fabricated to support research on the interaction of materials with inverted pyramids etched into silicon. The fabrication begins by depositing a thin layer of SiO_2 on a (100) silicon wafer. A tri-layer resist stack is deposited on the substrate, and the resist is patterned by interference lithography, in this case using the Lloyd's mirror IL system. Following development of the exposed resist, the pattern is transferred to the substrate using reactive-ion-etching, forming a grid of holes in the SiO_2 layer. The Si substrate is then etched in KOH, which preferentially etches into the $\langle 100 \rangle$ direction much faster than into the $\langle 111 \rangle$ direction, resulting in the formation of inverted-pyramids where each of the holes in the SiO_2 was located. Various materials can then be deposited or grown on the patterned substrate to determine how the surface patterning affects the material response.

A second set of substrates was fabricated for use in experiments on nanoporous aluminum oxide, which is formed by oxidizing aluminum under certain conditions. The process leads to the formation of many nanoscale pores perpendicular to the surface which generally have some characteristic spacing, but no long-range order. To provide long-range order in the pattern of pores, a silicon-rich silicon-nitride membrane was patterned using interference lithography. Reactive-ion-etching and liftoff were used to form an array of chromium cones on the membrane. By pressing the membrane into an aluminum surface with air-pressure on the backside the cones could be used to form small dents in the surface to determine if that would affect the location of the pores that would form when the aluminum was later oxidized.

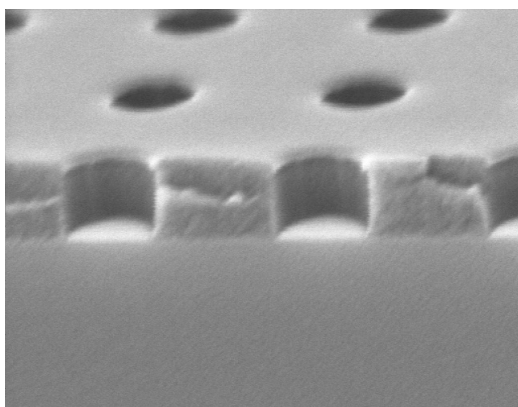


Figure 1: Micrograph of a stage in the preparation of a substrate containing an array of inverted-pyramids, for use in research on templated self-assembly. A pattern consisting of a grid of holes, with a spatial period of 200 nm, was written using interference lithography and has been transferred to the substrate by reactive ion etching. Due to differences in the etch rates of different crystal planes, etching this substrate in KOH will form inverted pyramids in the silicon substrate.

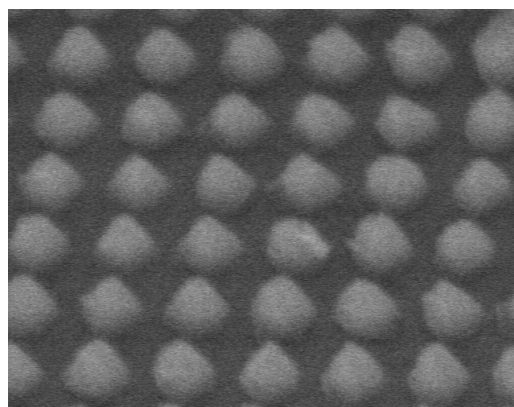


Figure 2: Micrograph showing a 200 nm-period grid of chrome cones on a silicon-nitride membrane. The pattern was created by interference lithography, and the cones were formed by a combination of etching and liftoff. These cones were formed for use in indenting an aluminum surface to control the positions of the pores in nanoporous aluminum oxide.

Publications

Journal Articles, Published

1. H-Y. Tsai, H. I. Smith, and R. Menon, "Fabrication of spiral-phase diffractive elements using scanning-electron-beam lithography," *J. Vac. Sci. Technol. B* 25(6), 2068-2071 (2007).
2. E.E. Moon, J. Kupec, M.K. Mondol, H.I. Smith, K.K. Berggren, "Atomic-force lithography with interferometric tip-to-substrate position metrology", *J. Vac. Sci. Technol, B* **25**, 2284 (2007).
3. Corey P. Fucetola, David J. Carter and James G. Goodberlet "Exposure latitude of deep-ultraviolet conformable contact photolithography", *J. Vac. Sci. Technol. B*26, 36-40 (2008).
4. Thomas B. O'Reilly and Henry I. Smith, "Photoresist characterization using double exposures with interference lithography," *J. Vac. Sci. Technol. B*, 26(1), 128-131 (2008)
5. Rajesh Menon, Hsin-Yu Tsai, Samuel W. Thomas III, "Far-Field Generation of Localized Light Fields using Absorbance Modulation," *Phys. Rev. Lett.*, 98, 043905 (2007).
6. Tymon Barwicz, Michael R. Watts, Miloš A. Popovic, Peter T. Rakich, Luciano Socci, Franz X. Kärtner, Erich P. Ippen, Henry I. Smith "Polarization-transparent microphotonic devices in the strong confinement limit," *Nature Photonics*, Vol. 1, Issue 1, pp. 57-60 (2007).
7. T. Barwicz, H. Byun, F. Gan, C.W. Holzwarth, M.A. Popović, P.T. Rakich, M.R. Watts, E.P. Ippen, F.X. Kärtner, H.I. Smith, J.S. Orcutt, R.J. Ram, V. Stojanović, O.O. Olubuyide, J.L. Hoyt, S. Spector, M. Geis, M. Grein, T. Lyszczarz and J.U. Yoon, "Silicon photonics for compact, energy-efficient interconnects (Inv.)," *J. Opt. Netw.* 6, 63-73 (2007).
8. W. J. Arora, H. I. Smith, G. Barbastathis, "Membrane folding by ion implantation-induced stress to fabricate three-dimensional nanostructures ," *Microelectronic Engineering* **84**, pp. 1454-1458 (2007).
9. F. Y. Ogrin, S.M. Weekes, B. Cubitt, A. Wildes, A. Drew, C.A. Ross, W. Jung, R. Menon," PNR investigation of periodic magnetic rings," *J. Appl. Phys.* In press (2007).
10. I. Bitá, T. Choi, M. E. Walsh, H. I. Smith and E. L. Thomas, "Large-area 3D Nanostructures with Octagonal Quasicrystalline Symmetry via Phase Mask Lithography," *Appl. Materials* **19**, 1403-1407 (2007).
11. H-Y Tsai, G. W. Wallraff, and R. Menon, "Spatial-frequency multiplication via absorbance modulation," *Appl. Phys. Lett.* 91(9), 094103 (2007).
12. H-Y. Tsai, H. I. Smith, R. Menon, "Fabrication of spiral-phase diffractive elements using scanning-electron beam-lithography," *J. Vac. Sci. Technol. B* **25**, pp. 2068-2071 (2007).
13. E. E. Moon, J. Kupec, M. K. Mondol, H. I. Smith and K. K. Berggren, "Atomic-force lithography with interferometric tip-to-substrate position metrology," *J. Vac. Sci. Technol. B* **25**, pp. 2284-2287 (2007).
14. C. Holzwarth, T. Barwicz and H. I. Smith, "Optimization of hydrogen silsesquioxane films for photonic applications," *J. Vac. Sci. Technol. B* **25**, pp. 2658-2661 (2007).

15. T. B. O'Reilly and H. I. Smith, "Characterization of photoresist using double-exposure with interference lithography," *J. Vac. Sci. Technol. B* 26, 128 (2008).
16. W. J. Arora, S. Sijbrandij, L. Stern, J. Notte, H. I. Smith and G. Barbastathis, "Membrane folding by He⁺ ion implantation for three-dimensional device fabrication," *J. Vac. Sci. Technol. B*, 2184-2187 (2007).
17. A. A. Patel and H. I. Smith, "Membrane stacking: A new approach for three-dimensional nanostructure fabrication," *J. Vac. Sci. Technol. B* 25, pp 2662-2664 Nov/Dec (2007).

Journal Articles, Submitted for Publication

1. R. Menon, P. Rogge, and H-Y. Tsai, "Design of diffractive lenses that generate optical nulls without phase singularities" submitted to *J. Opt. Soc. Am. A*.
2. "Accurate Frequency Alignment in Fabrication of High-order Microring-resonator Filters", J. Sun, C. W. Holzwarth, M. Dahlem, J. T. Hastings, submitted to *Optics Express*
3. Thomas B. O'Reilly and Henry I. Smith, "Linewidth Uniformity in Lloyd's Mirror Interference Lithography Systems", submitted to *J. Vac. Sci. Technol. B*

Conference Presentations

1. M.A. Popović, T. Barwicz, P.T. Rakich, M.S. Dahlem, C.W. Holzwarth, F. Gan, L. Socci, M.R. Watts, H.I. Smith, F.X. Kärtner and E.P. Ippen, "Experimental demonstration of loop-coupled microring resonators for optimally sharp optical filters," scheduled for presentation at the Conference on Lasers and Electro-Optics (CLEO), San Jose, CA, May 6, 2008, paper CTuNN3.
2. Charles W. Holzwarth, Jason S. Orcutt, Hanqing Li, Milos A. Popovic, Vladimir Stojanovic, Judy L. Hoyt, Rajeev J. Ram, Henry I. Smith, "Localized Substrate Removal Technique Enabling Strong-Confinement Microphotonics in Bulk Si CMOS Processes," to be presented at the Conference on Lasers and Electro-Optics
3. R. Menon, H-Y Tsai, H. I. Smith, "Patterning and Imaging at the nanoscale with far-field optics via absorbance modulation," *Technical Digest Photoninc metamaterials* (2007).

Thesis

1. H-Y. Tsai, Absorbance Modulation Optical Lithography, S.M. thesis, Department of Electrical Engineering and Computer Science, MIT, 2007.